

# Electrical and Optical Properties of Polymer-Au Nanocomposite Films Synthesized by Magnetron Cosputtering

Fanjung Liu,<sup>1</sup> Songmin Shang,<sup>2</sup> Yajun Duan,<sup>1</sup> Liang Li<sup>1,2</sup>

<sup>1</sup>Key Laboratory for Green Chemical Process of Ministry of Education, School of Materials Science and Engineering, Wuhan Institute of Technology, Wuhan 430073, China

<sup>2</sup>Institute of Textiles and Clothing, The Hong Kong Polytechnic University, Hong Kong, China

Received 18 April 2010; accepted 19 April 2011

DOI 10.1002/app.34723

Published online 1 September 2011 in Wiley Online Library (wileyonlinelibrary.com).

**ABSTRACT:** Polymer-Au nanocomposite films were prepared by co-sputtering from two independent magnetron sources. By sputtering from gold and polytetrafluoroethylene (PTFE) magnetrons, we prepared homogenous composite films using a rotatable sample holder. The microstructure of the nanocomposites was studied by transmission electron microscopy (TEM). The resistivity drops from  $10^7$  to  $10^{-3}$  Ohm cm over a narrow range of metal content. The thin

composite films show a strong optical absorption in the visible region due to surface plasmon resonances. The optical absorption has a strong dependence on the metal content, showing a red shift of the absorption peak from 550 nm to more than 700 nm with increasing gold content. © 2011 Wiley Periodicals, Inc. *J Appl Polym Sci* 123: 2800–2804, 2012

**Key words:** nanocomposite; PTFE; gold; threshold

## INTRODUCTION

Nanocomposite polymeric films combine the attractive functional properties of nanoparticles with the advantages of polymers, such as low cost and easy processability.<sup>1</sup> The electrical,<sup>2</sup> optical,<sup>3</sup> catalytic,<sup>4</sup> and antibacterial properties<sup>5</sup> are enhanced by adding metal nanoparticles to polymers. Thus polymer-metal nanocomposites are potential materials to produce effective optically and electrically active media. The properties of the nanocomposites depend on the amount, shape, size, and the spatial distribution of the metal nanoparticles in the polymer matrix, as well as on the polymer matrix itself.<sup>6,7</sup> Particularly near the percolation threshold, small changes in the arrangement of the nanocomposites can result in

dramatic changes in the electrical and optical properties of the material, which gives the possibility of applications in sensors and switching devices.

Consequently, various approaches such as reduction of a metal salt,<sup>8</sup> ball milling,<sup>9</sup> plasma polymerization techniques,<sup>10</sup> and coevaporation of a metal and an organic component<sup>11,12</sup> have been reported to produce metal nanoparticle-containing polymer-based composites. Physical vapour deposition (PVD) techniques (evaporation, sputtering, and other hybrid and modified PVD processes) are promising methods used for the preparation of nanocomposite films in a dry process. The technological advantage of the PVD technique is excellent conformity over complex topography. The possibility of a uniform composite film on relative large substrate is also realizable. The technological advantage of the sputter technique over other techniques is the possibility to realize a higher deposition rate, as demonstrated by RF magnetron deposition of different polymers. Additionally, there are no problems with residual solvents as in wet chemical synthesis processes.

In this work, we used a PVD technique based on cosputtering gold and polymer from independent magnetron sources. High deposition rates can be realized with this sputter technique. Polytetrafluoroethylene (PTFE) was chosen as a polymer matrix due to its known properties of high resistance to any chemical attack and excellent dielectric properties. The emphasis in this article is placed on the dependence of the optical and electrical properties especially near the percolation threshold on metal content and preparation conditions. The effect of post deposition annealing on their optical properties was also studied.

Correspondence to: S. Shang (tcshang@inet.polyu.edu.hk) and L. Li (msell08@163.com).

Contract grant sponsor: Educational Bureau of Hubei Province; contract grant number: Q20091508.

Contract grant sponsor: Scientific Research Key Project of Ministry of Education of China; contract grant number: 209081.

Contract grant sponsor: National Natural Science Foundation of China; contract grant number: 20904044.

Contract grant sponsor: Hong Kong Innovation Technology Fund; contract grant number: ITS/003/09.

Contract grant sponsor: The Hong Kong Polytechnic University; contract grant number: A-PK10.

Contract grant sponsor: the New Century Excellent Talents in University, Ministry of Education, China; contract grant number: NCE1-10.

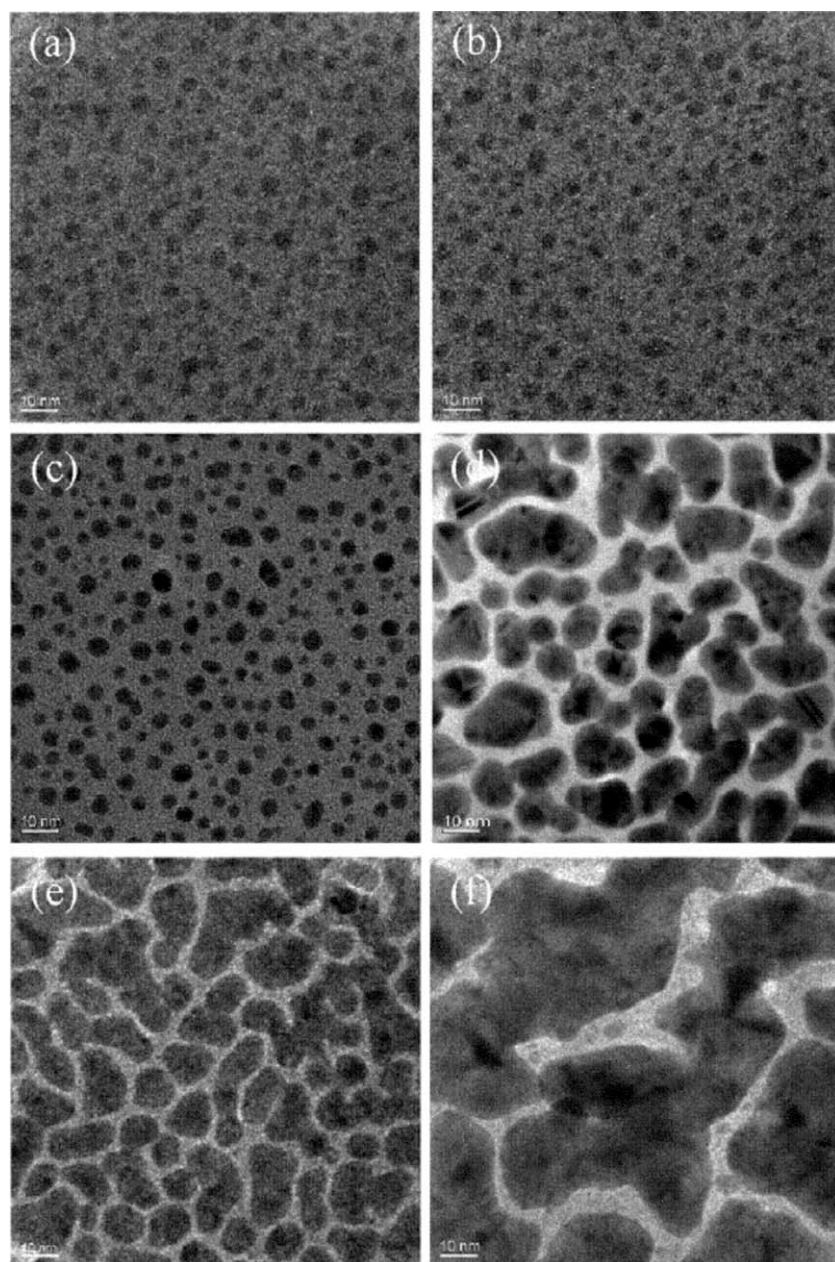


**Figure 1** TEM micrographs of the nanocomposites with different gold contents, (a) 0.10, (b) 0.16, (c) 0.24, (d) 0.34, (e) 0.43, and (f) 0.54.

## EXPERIMENTAL

### Materials

Gold (99.99% pure, metallic wire) and PTFE were purchased from Good Fellow Industries, UK and Aldrich, respectively, and used as received.

### Synthesis of PTFE-Au nanocomposite films by magnetron cosputtering

Composite film coatings were prepared by simultaneous sputtering of polymer and metal from independent magnetron sources on the substrate. All experiments were carried out in a metal vacuum chamber, which

was initially evacuated to a pressure below  $10^{-7}$  Torr. The RF magnetron system for sputtering PTFE and DC magnetron sputter source for gold were used. Both polymer and Au targets with a diameter of 2 inches were mounted on a cooled holder. The magnetrons were arranged from opposite direction with an angle of  $50^\circ$  to the substrate. Normally an RF power of 50 W was applied to the PTFE target and a DC power of 10 W was applied to the gold target. Quartz-crystal monitors were installed in the chamber to control the deposition rates of Au and PTFE, which allowed the synthesis of the nanocomposite films with different contents of metal. The metal content and the deposition rate could also be adjusted by changing the deposition parameters

such as the input power and the sputter gas (argon) pressure. By increasing the input power the deposition rate of the polymer increased faster than the metal rate and the metal content decreased, whereas an increase of the pressure had the opposite effect. We could control the metal content by adjusting the deposition ratio of the metal and the polymer from the two sputter sources. To obtain the films with a uniform thickness and the homogeneous gold spatial distribution a rotatable sample holder was used. Thickness measurements show only a difference of a few percent over the sample area.

### Characterization

For the characterization of a PTFE–Au nanocomposite, we determined the content of metal nanoparticles in the nanocomposite films, which was specified as a volume filling factor  $f$

$$f = \frac{\frac{m}{V} - \rho_p}{\rho_m - \rho_p} \quad (1)$$

where  $\rho_p$  is the density of the polymer host,  $\rho_m$  is the density of the metal,  $m$  is the mass, and  $V$  is the volume of the nanocomposite film, which was determined by the measurement of the film thickness and a sample area. The thickness of the nanocomposite films was measured with a profilometer (Dektak 8000 surface profile measuring system). Layers of the composite films with a maximum thickness of 100 nm were deposited on glass slides for UV–VIS measurements. The optical properties were studied using an UV/VIS/NIR-spectrometer Lambda 900 (Perkin Elmer). Substrates with evaporated aluminium contacts were used to study the electrical properties. The conductivities of the nanocomposite films were measured with a Keithley Model 6485 picoammeter. To obtain information about the morphology of the nanocomposites, TEM micrographs (Philips CM 30 TEM) were taken after deposition of the nanocomposite films on carbon-covered copper grids.

## RESULTS AND DISCUSSION

The polymer–metal composite films prepared by cosputtering of both components show a morphology in which the metal nanoparticles are uniformly dispersed in a polymer matrix. One can assume that the formation of metal nanoclusters in a polymer matrix can be described in the same way as for cluster formation on the polymer surface.<sup>13</sup> When energetic metal atoms impinge on the polymer surface, which grows simultaneously by polymer fragment deposition and repolymerization, the arriving metal atoms undergo various processes, namely random walk on the polymer surface, diffusion into the grown polymer or desorption. Within the diffusion distance, metal atoms may encounter

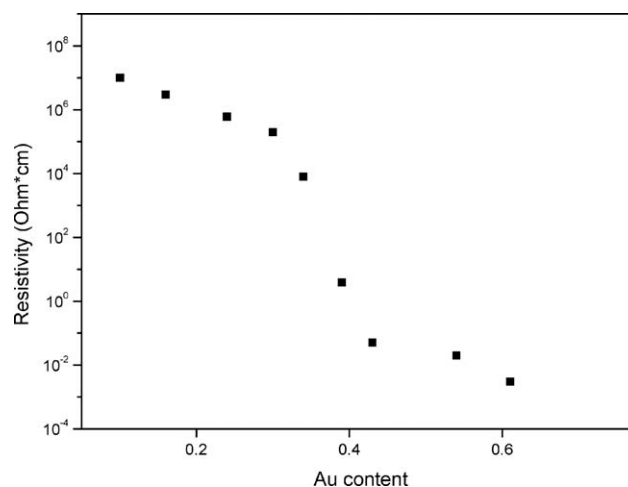


**Figure 2** Resistance change with increasing amount of gold.

each other or are captured by a surface site. This leads to aggregation and formation of stable metal clusters in the polymer. Figure 1 shows the TEM images of PTFE–Au nanocomposite films with different metal content. The microstructure of the nanocomposites can be controlled by the deposition parameters such as the specific deposition rate. When the content of gold is small [Fig. 1(a)], gold nanoparticles with the size distribution of 3–7 nm are isolated from each other without the formation of a continuous network. However, the gold nanoparticles become larger with the increase of the amount of gold, get closer to each other as showed in Figure 1(d), and even finally could form conductive channels.

The nanocomposite films deposited with varying metal content show large variations in electrical and optical behaviors. On the basis of the metal content in the nanocomposites, the electrical properties can be distinguished into three different regions: the dielectric, percolation (transition) and metallic region. The character of the electrical transport depends on the film composition and the separation between metal nanoparticles.<sup>14</sup> The percolation region refers to the transition between a microstructure of separate metal particles inside the polymer matrix and a network of interconnected clusters. Near the percolation threshold, the possibility of electron tunneling between neighboring particles as well as the formations of metal chains and conducting channel are given.<sup>15</sup> Therefore, the electrical properties changes dramatically over a small composition range. The electrical properties of the nanocomposites as a function of the Au content are presented in Figure 2. The resistances of the nanocomposite film drops by several orders of magnitude at a metal content of about 0.39. This is in agreement with the various theoretical values for the



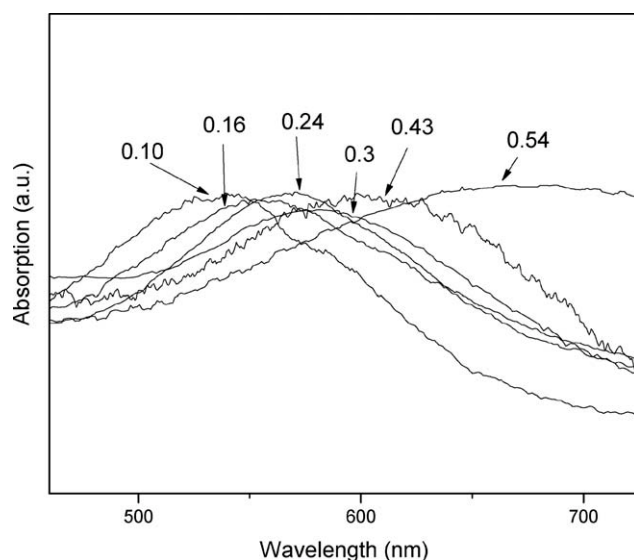


**Figure 3** UV-vis spectra of the nanocomposites with different gold content.

percolation threshold for spherical clusters given in the literatures, ranging between 0.28 and 0.50.<sup>16</sup>

The optical properties of the nanocomposite films were also studied as a function of the metal content using an UV/VIS/NIR-spectrometer. We observed a red shift in the UV-vis spectra that the absorption maximum from 540 nm for small metal content shifts to more than 680 nm for metal content above the percolation threshold (Fig. 3). There was only a slight shift of the particle plasmon resonance frequency observed for small metal content. Near the percolation, a stronger dependence of the resonance frequency on the metal content was observed. With increasing metal concentration in the composite film near the percolation threshold the gaps between single clusters become smaller and the cluster size and

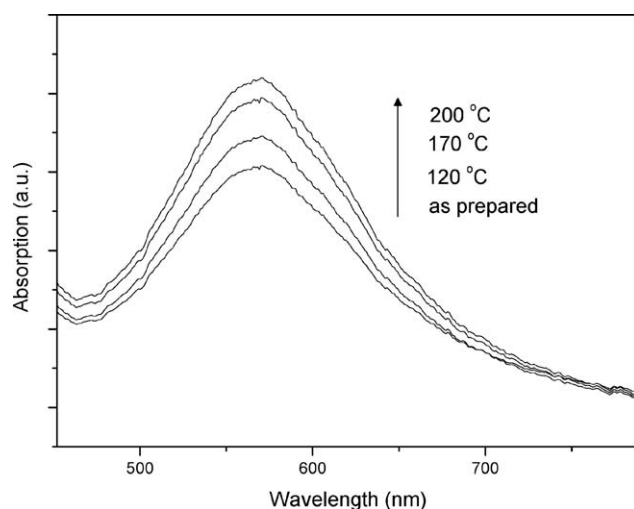


**Figure 4** UV-vis spectra of the nanocomposite annealed at various temperatures for 10 min.

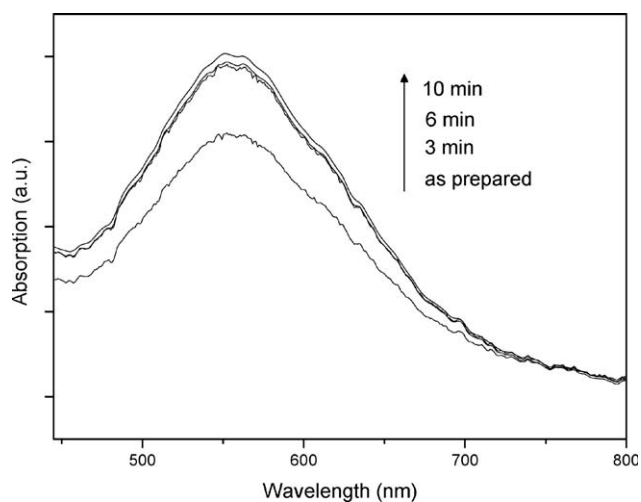


**Figure 5** UV-vis spectra of the nanocomposite annealed at 160 °C for different times.

shape can also change due to coalescence of the particles. The resulting significant red shift of the absorption maximum is in good agreement with theoretical models.<sup>7</sup> Furthermore, a broadening effect of the absorption peak occurs at higher metal content (larger than the values of the percolation threshold), because of the wider size distribution and more irregular shape of the metal clusters.

There are also different ways to change the microstructure of the nanocomposites after deposition such as thermal annealing, X-ray irradiation and electron beam heating.<sup>17</sup> Here, we changed the optical absorption in the visible region caused by thermal annealing in air of the nanocomposites. Annealing results in a heat-induced size evolution of small gold nanoparticles in the film and structural relaxation of the polymer matrix.<sup>18</sup> Figure 4 shows UV-vis spectra of a PTFE-Au nanocomposite (metal content is about 0.24) annealed at various temperatures. The intensity of the absorption peak increases with higher annealing temperature, while there is no shift in position of the absorption peak, which indicates the absence of significant change in the metal content. No shift of the plasmon band of the clusters indicates that the red shift of the band caused by a growth of the clusters is similar with the blue shift caused by the increase in the particle distance. Figure 5 shows UV-vis spectra of a PTFE-Au nanocomposite (metal content is about 0.16) during heat treatment at 160 °C for different times. It is possible to transform the initial metastable structure of the nanocomposites to a more stable structure by heat treatment. It is observed that there are no significant changes of the intensity of the absorption peaks for heat treatments longer than 3 min. It implies that metal clusters are immobile once they attain the lower surface energy to be in an equilibrium state.<sup>19</sup>

## CONCLUSIONS

In summary, nanocomposites with different optical and electrical properties containing gold nanoparticles embedded in PTFE matrix were successfully fabricated by sputtering from two independent magnetron sources in a dry system. The relatively high deposition rates and an uniformity of the deposited films can be obtained by sputtering technique. It is shown that the electrical and optical behaviors of the nanocomposites are influenced by their microstructure parameters. The optical absorption peak due to the particle plasmon resonance is shifted to higher wavelength with the increase in the filling factor of the metal. Moreover, the shift of the plasmon peak is more pronounced for high filling factors due to an increase in the size of the clusters and a decrease in the distance between neighbouring clusters. The electrical behaviors also depend on the microstructural parameters mainly on the content of metal in the nanocomposites and change drastically from insulating to metallic near the percolation threshold.

## References

1. Faupel, F.; Zaporojtchenko, V.; Greve, H.; Schurmann, U.; Chakravadhanula, V. S. K.; Hanisch, Ch.; Kulkarni, A.; Gerber, A.; Quandt, E.; Podschun, R. *Contrib Plasma Phys* 2007, 47, 535.
2. Ajayan, P. M.; Schadler, L. S.; Braun, P. V. *Nanocomposite Science and Technology*; Weinheim: Wiley-VCH, 2003.
3. Biswas, A.; Aktas, O. C.; Schumann, U.; Saeed, U.; Zaporojtchenko, V.; Faupel, F.; Strunskus, T. *Appl Phys Lett* 2004, 84, 2655.
4. Lewis, L. N. *Chem Rev* 1993, 93, 2693.
5. Zaporojtchenko, V.; Podschun, R.; Schurmann, U.; Kulkarni, A.; Faupel, F. *Nanotechnology* 2006, 17, 4904.
6. Kelly, K. L.; Coronado, E.; Zhao, L. L.; Schatz, G. C. *J Phys Chem B* 2003, 107, 668.
7. Kreibitz, U.; Vollmer, M. *Optical Properties of Metal Clusters*; Springer: Berlin, 1995.
8. Troger, L.; Hunnefeld, H.; Nunes, S.; Oehring, M.; Fritsch, D. *J Phys Chem B* 1997, 101, 1279.
9. Giri, A. K. *J Appl Phys* 1997, 81, 1348.
10. Martinu, L.; Biderman, H. *Plasma Chem Plasma Process* 1985, 5, 81.
11. Boonthanom, N.; White, M. *Thin Solid Films* 1974, 24, 295.
12. Biswas, A.; Marton, Z.; Kruse, J.; Kanzow, J.; Zaporojtchenko, V.; Faupel, F.; Strunskus, T. *Nano Lett* 2003, 3, 69.
13. Zaporojtchenko, V.; Behnke, K.; Thran, A.; Strunskus, T.; Faupel, F. *Appl Surf Sci* 1999, 144–145, 355.
14. Ung, T.; Liz-Marzan, L. M.; Mulvaney, P. *J Phys Chem B* 2001, 105, 3441.
15. Schurmann, U.; Hartung, W.; Takele, H.; Zaporojtchenko, V.; Faupel, F. *Nanotechnology* 2005, 16, 1078.
16. Sheng, P. *Phys Rev B* 1980, 21, 719.
17. Heilmann, A.; Werner, J.; Stenzel, O.; Homilius, F. *Thin Solid Films* 1994, 246, 77.
18. Teransishi, T.; Hasegawa, S.; Shimizu, T.; Miyake, M. *Adv Mater* 2001, 13, 1699.
19. Iwamoto, M.; Kuroda, K.; Zaporojtchenko, V.; Hayashi, S.; Faupel, F. *Eur Phys J D* 2003, 24, 365.